Industrial Crops & Products 126 (2018) 22–30

Contents lists available at ScienceDirect

Industrial Crops & Products

journal homepage: www.elsevier.com/locate/indcrop

Optimization and kinetic modelling of robinetin and dihydrorobinetin extraction from *Robinia pseudoacacia* wood

Stéphane Bostyn[a,b,*], Emilie Destandau[c], Jean-Paul Charpentier[d,e], Valérie Serrano[f], Jean-Marc Seigneuret[f], Christian Breton[d]

[a] Institut de Combustion, Aérothermique, Réactivité, et Environnement (ICARE)-CNRS UPR3021, 1C avenue de la recherche scientifique, 45071 Orléans Cedex 2, France
[b] University Orléans, IUT d'Orléans, 45067 Orléans, France
[c] University Orléans, CNRS, ICOA, UMR 7311, 45067 Orléans, France
[d] INRA Val de Loire, BioForA, UMR 0588, 45075 Orléans, France
[e] GénoBois Wood Analysis Platform, INRA Val de Loire, 45075 Orléans, France
[f] Alban Muller International, Fontenay-sur-Eure, France

ARTICLE INFO

Keywords:
Extraction
Flavonoid
Robinetin
Dihydrorobinetin
Robinia pseudoacacia
Kinetic model

ABSTRACT

Due to its rapid growth and important biomass production abilities, black locust (*Robinia pseudoacacia* L.) wood could represent an interesting source of natural compounds. Here, we optimized the extraction of the two main flavonoids accumulated in this species wood (i.e.: robinetin and dihydrorobinetin) with 80:20 (w:w) ethanol:-water solvent well adapted for further industrial uses such as cosmetics. Our experimental design focused on two main extraction parameters: temperature and wood/solvent volume ratio that were optimized to 27.5 °C and 177 g L^{-1}, respectively. These conditions lead to an optimal recovery of about 3000 mg L^{-1} of dihydrorobinetin and 700 mg L^{-1} of robinetin in the extracts. Interestingly, the effect of temperature could be neglected allowing reduced energy consumptions at the industrial level. Analysis of the evolution of robinetin and dihydrorobinetin concentrations during the timespan of the experiments revealed similar behaviours for both molecules. Kinetic modelling of robinetin and dihydrorobinetin release showed that pseudo-second order rate laws described well the extraction process with r^2 values over 0.91. In the end, the results of this study provided useful insights to scale-up the extractions and lead to an industrial production of black locust wood extracts enriched in both flavonoids of interest.

1. Introduction

Since its introduction in France by Jean Robin in 1601, black locust (*Robinia pseudoacacia*) has spread within the temperate regions of most continents. Characterized by rapid growth rates, important flowering and seed production abilities, this species also proved to be well adapted to a wide range of environmental conditions and became the third hardwood tree species harvested worldwide for its wood (Barbier et al., 2016). Compared to poplars and eucalyptus, black locust wood is characterized by very high natural durability ratings (Scheffer and Cowling, 1966). Hence, besides being advantageously logged for energy production, its timber is also particularly appreciated for outdoor uses as fence posts, furniture, decking, and cladding. Considered in Europe as a dangerous invasive species (Weber and Gut, 2004; Benesperi et al., 2012), it is commonly represented all over the French and European territories and its wood could represent an interesting sourcing of natural compounds.

In many hardwood species, different flavonoid subclasses of polyphenols have been linked to wood color and heartwood natural durability properties (Hillis, 1987). Accumulated in large quantities in the wood, they often present interesting antioxidant and antimicrobial properties (George et al., 2017). In *R. pseudoacacia*, dihydrorobinetin (DHR) and Robinetin (Rob) are the two major flavonoids detected in wood extractives (Magel et al., 1994; Sergent et al., 2014; Magel, 2000). Interestingly, these extracts presented some antifungal properties and Rob was also shown to present fluorescent properties (Shain, 1977; Guharay and Sengupta, 1997). Due to both of these properties, it seemed interesting to prospect the use of black locust wood as source of bioactive extracts for cosmetics. In the end, these extracts or molecules could be used as natural dye or preservative. Polyphenol extractions are

* Corresponding author at: Institut de Combustion, Aérothermique, Réactivité, et Environnement (ICARE)-CNRS UPR3021, 1C avenue de la recherche scientifique, 45071 Orléans Cedex 2, France.
E-mail address: stephane.bostyn@univ-orleans.fr (S. Bostyn).

https://doi.org/10.1016/j.indcrop.2018.09.049
Received 25 April 2018; Received in revised form 21 September 2018; Accepted 24 September 2018
Available online 06 October 2018

generally achieved at various temperatures and with solvent mixtures based on large ranges of ethanol and water ratios. Jurinjak Tušek et al. (2016) used deionized water at temperatures varying between 40 °C and 80 °C whereas Mkaouar et al. (2016) used 95% ethanol at 55 °C. In *R. pseudoacacia*, wood macerations have already been described with different solvents (80% acetone, 50% ethanol or methanol mixtures) and experimental conditions (40 °C, 4 h or 20 °C, 24 h) (Magel et al., 1994; Sanz et al., 2011; Sergent et al., 2014; Destandau et al., 2016). These studies aimed at determining wood phenolic compound and flavonoid contents linked to heartwood formation. In the present work, acetone and methanol were not considered since the extracts could potentially be used as colorant or natural protective phytochemical for pharmaceutics, cosmetics and/or phytosanitary industries. Hence, we focused on the optimization of Rob and DHR extraction conditions and on modeling their kinetics. A design of experiment (DoE) was set-up to generate polynomial models and response surfaces in order to define the optimal extraction conditions. Three-level factorial, Box–Behnken, central composite, and Doehlert experimental designs may be used to address such models (Bezerra et al., 2008). Indeed, the extractions of different polyphenols have already been described through three-level factorial designs (Sant'Anna et al., 2012; Odabaş and Koca, 2016; Katsampa et al., 2015). Interestingly, Doehlert designs allow the determination of a second-order model based on response surface methodology with a minimum number of experiments (Chartier et al., 2013; Moreno-Vilet et al., 2014).

In this paper, we also took advantage of the Doehlert design to apply the simplex methodology that allows the initial experimental domain to be extended in order to determine an optimal value for each studied parameter. In the end, our goal was to propose the most efficient and cost-effective process of extraction in order to insure an industrial transfer. Considering wood sawdust as starting material, we directed our experiments towards a traditional liquid–solid extraction and optimized the extraction conditions through a Doehlert design focused on two main parameters: temperature and solid/solvent mass volume ratio. Based on the results of this approach, DHR and Rob extraction kinetics were determined and lead us to successfully transfer the extraction process to a pre-industrial level.

2. Materials and methods

2.1. Materials, reagents and extract analysis

R. pseudoacacia wood particles used for extraction optimization and kinetic analysis were obtained and prepared as in Destandau et al. (2016). The majority of wood particle was sized between 0.4 and 1 mm. Thinner wood particles were sieved out in order to avoid clogging during the solid/liquid filtering step allowing the recovery of the extracts. Ethanol, methanol, acetonitrile (analytical reagent grade, VWR, Fontenay-sous-Bois, France) and purified water (Elgastat UHQ II system, Elga, Antony, France) were used for extractions and analysis. Robinetin (Rob) and dihydrorobinetin (DHR) (Extrasynthese, Genay, France) were purchased as standards for calibration curves establishment.

The wood used for industrial trials (400 kg of wood pellets) was obtained and prepared through a local (< 200 km) chain of suppliers and manufacturers established in collaboration with the Arbocentre association (Orléans, France). Industrial pilot extractions (50 kg of wood particles) were realized at Alban Müller International facilities (Fontenay-sur-Eure, France).

For each experimental point, the contents of DHR and Rob were determined by HPLC analysis of extract aliquots as in Destandau et al. (2016). Five diluted solutions of DHR and Rob (10 mg L^{-1} to 500 mg L^{-1}) were injected to determine both calibration curves: YRob = 22.084x + 91.996 (r^2 = 0.9997) and YDHR = 46.165x − 254.45 (r^2 = 0.9992) used to estimate their amounts within the extracts.

2.2. Rob and DHR extraction

Solid–liquid extractions were performed in a 1.5 L batch reactor equipped with a HUBER ministat thermocryostat and an IKA EUROSTAR stirring system (Fischer Scientific, Illkirch, France) to precisely control the temperature and provide constant homogenization during maceration. The stirring was set at 250 rpm. During the optimization process, solvent mass was kept at 300 g (corresponding to 356 mL at 20 °C) while the mass of wood matter to be extracted was adjusted to the different wood/solvent mass ratios selected. For each condition, extract aliquots of 5 mL were collected every hour until 4 h in order to determine Rob and DHR concentrations and their kinetics of extraction.

2.3. Doelhert experimental design

To optimize solid–liquid extraction of DHR, five parameters had previously been studied: solvent nature, solid granulometry (wood particle size), temperature (T), solid/solvent weight ratio (R) and, residence time (t) (Destandau et al., 2016). Based on these results, only temperature and solid/solvent weight ratio have been retained as parameters for the design of experiment (DoE) of the present study. The chosen solvent is a mixture of ethanol and water at 80:20, respectively. For response surface methodology, a Doehlert experimental design was chosen as it requires less experiments to estimate the terms of a second-order equation (Eq. (1)) model for two independent parameters (Chartier et al., 2013). According to this design, only six experiments are required to determine the terms of this equation and three additional repeats are generally performed in the domain center in order to estimate the experimental errors. In the end, the experimental points define a sphere in which each parameter is analyzed at different level numbers according to its influence on the extraction (Fig. 1; Table 1). For each parameter, the number of levels is mainly dependent upon the possibility to precisely control its value and its influence on the extraction. T was studied at 5 levels between 15 and 40 °C and R at 3 levels (i.e.: 0.01, 0.05 and 0.09 g/g corresponding to 84.3, 42.15 and 75.87 g L^{-1} respectively) and two responses were followed, i.e.: Rob concentration (C_{rob}) and DHR concentration (C_{dhr}). According to Eq. (1), the experimental results will allow the estimation of six coefficients corresponding to the following second-order polynomial model in which the two independent and studied variables are represented by X_1 (T) and X_2 (R).

$$Y = b_0 + b_1X_1 + b_2X_2 + b_{11}X_1^2 + b_{12}X_1X_2 + b_{22}X_2^2 \quad (1)$$

This model is defined by first-order terms (b_i), square terms (b_{ii}) and first-order interaction term (b_{ij}). The coefficients of the polynomial model (b_0, b_i, b_{ii} and b_{ij}) were estimated through the least-square method (Statgraphics Centurion, XVI Version Software, Sigma-Plus,

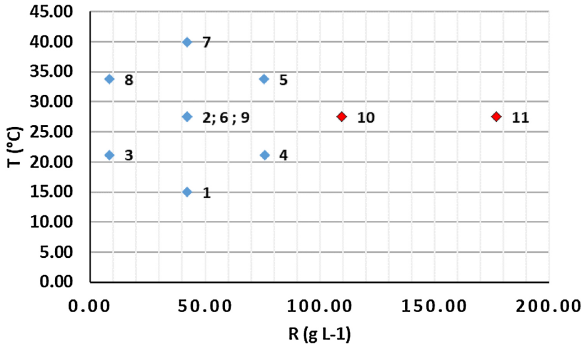

Fig. 1. Graphical representation of the Doelhert design summarizing the different experimental conditions tested to optimize the extraction of dihydrorobinetin (DHR) and Robinetin (Rob) from black locust wood (◆). The Doelhert plan is then extended through the simplex method given experiments 10 and 11 (◆).

Table 1
Doehlert matrix design (1 to 9) and simplex experiments (10 to 11) with experimental results.

Experiment number	T (°C)	R (g g^{-1}; g L^{-1})	C_{DHR} (mg L^{-1})	C_{Rob} (mg L^{-1})	C_{pred} DHR[a] (mg L^{-1})	C_{pred} Rob[a] (mg L^{-1})
1	15.0 (−1)	0.05; 42.15 (0)	505.8	104.4	613.67	137.24
2	27.5 (0)	0.05; 42.15 (0)	748.3	172.0	688.10	156.88
3	21.2 (−0.5)	0.01; 8.43 (−0.866)	119.1	30.8	69.73	12.16
4	21.2 (0.5)	0.09; 75.87(+0.866)	1281.4	300.6	1232.03	281.96
5	33.8 (+0.5)	0.09; 75.87 (0.866)	1089.8	233.5	1190.27	265.29
6	27.5 (0)	0.05; 42.15 (0)	770.8	175.1	688.10	156.88
7	40 (+1)	0.05; 42.15 (0)	804.5	194.1	762.53	176.51
8	33.8 (+0.5)	0.01; 8.43 (−0.866)	159.9	36.3	260.37	68.09
9	27.5 (0)	0.05; 42.15 (0)	713.3	165.1	688.10	156.88
10	27.5 (0)	0.13; 109.59 (2)	1782.1	398.4	–	–
11	27.5 (0)	0.21; 177.03 (4)	2997.3	671.2	–	–

In brackets, reduced coordinates of each experiment.
[a] Values calculated with model.

Paris, France). Each term was validated by *F*-tests with a probability of 95% ($p = 0.05$) on mean squares. Once defined, the equation is used to establish the response surface.

On a practical point of view, the temperature range of study was defined by the fact that the results could be implemented for industrial use. Temperature being a costly feature in industrial process, a lower limit of 15 °C was chosen to minimize future energy consumption. On the opposite, the upper level was defined to reduce the possibility of thermal degradation of the target molecules. Preliminary experiments proved that no degradation of Rob and DHR were observed after the extracts were submitted to 8 h of heating at 50 °C. Based on these results, the upper temperature limit of the experimental design was set at 40 °C.

2.4. Simplex method

The simplex method is a progressive experimental condition optimization method based on the removal of the worst experimental condition from the initially tested set that is then replaced by a new condition chosen in the opposite direction of the eliminated one. The process is repeated until optimal conditions are reached (Spendley et al., 2012; Bostyn et al., 2009; D'Attoma et al., 2017). In this process, the new condition to be tested (Xr,j) are calculated according to Eq. (2):

$$Xr, j = Xg, j + \alpha(Xg, j - Xw, j) \quad (2)$$

where Xr,j represents the reduced coordinates of the new point for the variable j, Xg,j the average levels of the remaining conditions, Xw,j the rejected condition and α an expansion or contraction coefficient chosen to determine the new point's coordinates.

2.5. Kinetic model

Two models were selected to establish correlations between the experimental data and a mathematical model in view to represent the evolution of Rob and DHR concentrations in the extract in function of time:

2.5.1. The pseudo-second order rate model

The kinetic models describing the evolution of Rob and DHR concentrations within time were determined according the pseudo-second order rate law described by Su et al. (2014). In brief, this model is based on the following general Eq. (3) that determines the extraction rate (mg L^{-1} min^{-1}) according to the extraction rate constant k (L mg^{-1} min^{-1}), the equilibrium concentration (C_e) of either Rob or DHR and their concentrations (C_t) in the suspension at any given extraction time (t):

$$\frac{dc_t}{dt} = k(C_e - C_t)^2 \quad (3)$$

When $t \approx 0$, the initial extraction rate (h) is defined with the Eq. (4):

$$h = k \cdot Ce^2 \quad (4)$$

The kinetic parameters h and k are then obtained by integrating Eq. (3) with t and C_t values ranging from 0 to t and 0 to C_t, leading respectively to Eqs. (5) and (6) after linearization:

$$c_t = \frac{c_e^2 kt}{1 + c_e kt} \quad (5)$$

$$\frac{t}{C_t} = \frac{1}{kC_e^2} + \frac{t}{C_e} = \frac{1}{h} + \frac{t}{C_e} \quad (6)$$

An equivalent formulation of Eq. (6) would be Eq. (7) as described by Jurinjak Tušek et al. (2016):

$$C_t = \frac{t}{K_1 + K_2 t} \quad (7)$$

This latest formulation represents the model developed by Peleg (1988) in which K_1 is Peleg's rate constant (related to the initial extraction rate) and K_2 represents Peleg's capacity constant corresponding to C_{rob} and C_{dhr} maximum values observed in the extracts for both molecules at the equilibrium.

2.5.2. Power law model

This model has been used by Sant'Anna et al. (2012) and Patil and Akamanchi (2017). Its mathematical form is represented by Eq. (8),

$$C_t = kt^{-n} \quad (8)$$

where C_t is the concentration either of DHR or Rob at a specific time (min), n a power law exponent, and k a constant related to the extraction (L mg^{-1} min^{-1}). The following linear form of Eq. (8) is

$$\ln c_t = \ln k - n \ln t$$

3. Results and discussion

3.1. Optimization of Rob and DHR extraction process

Rob and DHR concentrations measured after an extraction time of 4 h according to the Doelhert experimental design used are reported in Table 1 for each experiment number (1–9). In the studied domain, C_{rob} varied between 30.8 (Exp. 3) and 323.6 mg L^{-1} (Exp. 4) suggesting a range factor of 11 whereas C_{DHR} between 119.1 (Exp. 3) and 1379.8 (Exp. 4) for a range factor of 12. In general, one can extract four to five times more DHR than Rob. Interestingly, extreme results are observed for the same experiment number for both molecules. The same profile of concentration can also be observed according to each experiment number. This similitude of profile reveals equivalent behaviors for both molecules with respect to the studied parameters (T and R). Indeed, Fig. 2 highlights the close chemical relationship between Rob and DHR.

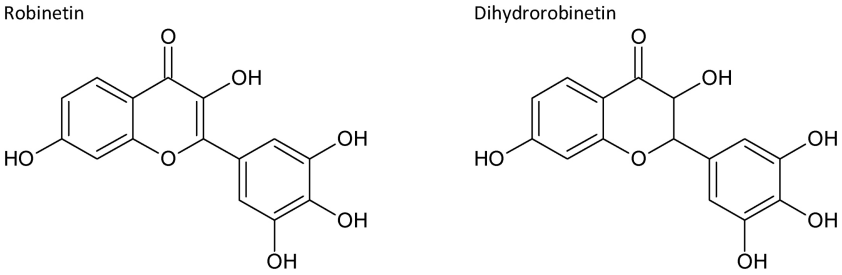

Fig. 2. Structures of *Robinia*'s major wood flavonoid molecules: robinetin (3,3′,4′,5′,7-Pentahydroxyflavone) (Rob), dihydrorobinetin (3,3′,4′,5′,7-Pentahydroxyflavanone) (DHR).

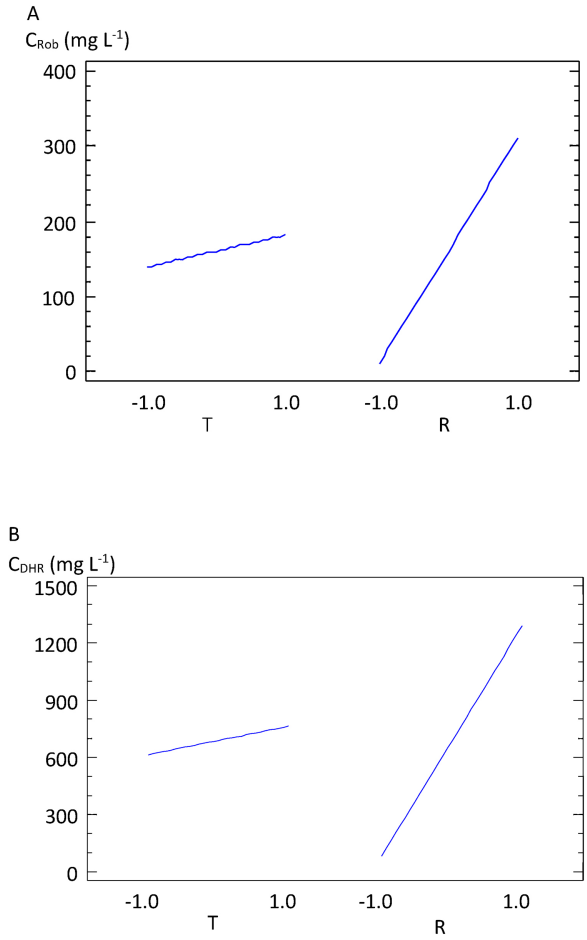

Fig. 3. Main effect plots for temperature (*T*) and solid/solvent weight ratio (*R*) on Robinetin (Rob) (A) and dihydrorobinetin (DHR) (B) extraction.

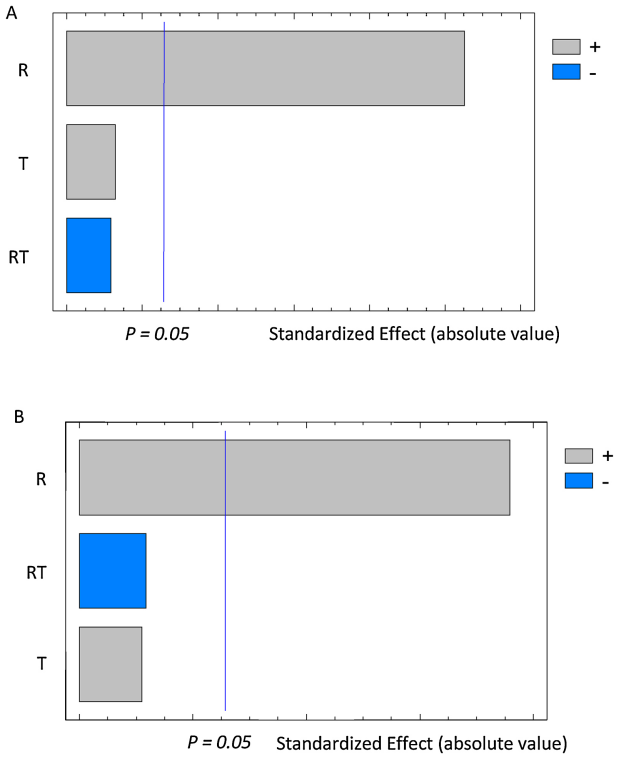

Fig. 4. Pareto diagrams describing the effects of *R* and *T* and their interactions (*RT*) on dihydrorobinetin (DHR) (A) and Robinetin (Rob) (B) concentrations.

Table 2
F-test results of the quadratic polynomial model variables influencing dihydrorobinetin (DHR) concentration in the extracts.

Source[a]	Sum of squares	Df	Mean square	*F*-ratio	*p*-Value
T	16,621.0	1	16,621.0	1.41	0.3205
R	1.09433E6	1	1.09433E6	92.86	0.0024
TT	9501.64	1	9501.64	0.81	0.4354
TR	13,502.4	1	13,502.4	1.15	0.3629
RR	7511.34	1	7511.34	0.64	0.4830
Total error	35,354.2	3	11,784.7		
Corrected total	1.174E6	8			

r^2 = 97.0%
r^2_{adj} = 92.0%
[a] Studied variables: temperature (*T*); solid/solvent weight ratio (*R*).

The only structural difference between both of these flavonoids corresponds to a double bond on position 2,3 for Rob.

The main effect graphics (Fig. 3) show the impact of both parameters on Rob and DHR concentrations. One can conclude for both molecules that each parameter has a positive effect on the extraction process with *R* being more important than *T*.

3.1.1. Optimization of DHR extraction

F-test results are reported in Table 2. Out of the two parameters tested, only *R* is significant for the extraction process of DHR (*p-value* < *0.05*). Therefore, unsignificant terms have been removed taking into account the evolution of the r^2 and r^2_{adj} values (Chartier et al., 2013). The maximal value of r^2_{adj} is 0.932 with a r^2 equal to 0.957 obtained with the following model: $C_{DHR} = 688.1 + 74.43T + 603.98R - 134.18RT$. With values higher than 0.8, the calculated regression coefficients suggest good correspondences between our experimental results and the predicted values (Odabaş and Koca, 2016). For this model, the standard error of estimate is 99.5 mg L^{-1} for C_{DHR}. Being superior to the confidence interval of 72.5 mg L^{-1} calculated with the Student tests applied to experiments: 2, 6, and 9 ($p < 0.05$ with degree of freedom = 2), it shows that the standard deviation of residues is greater than the experimental errors. The *F*-ratio between

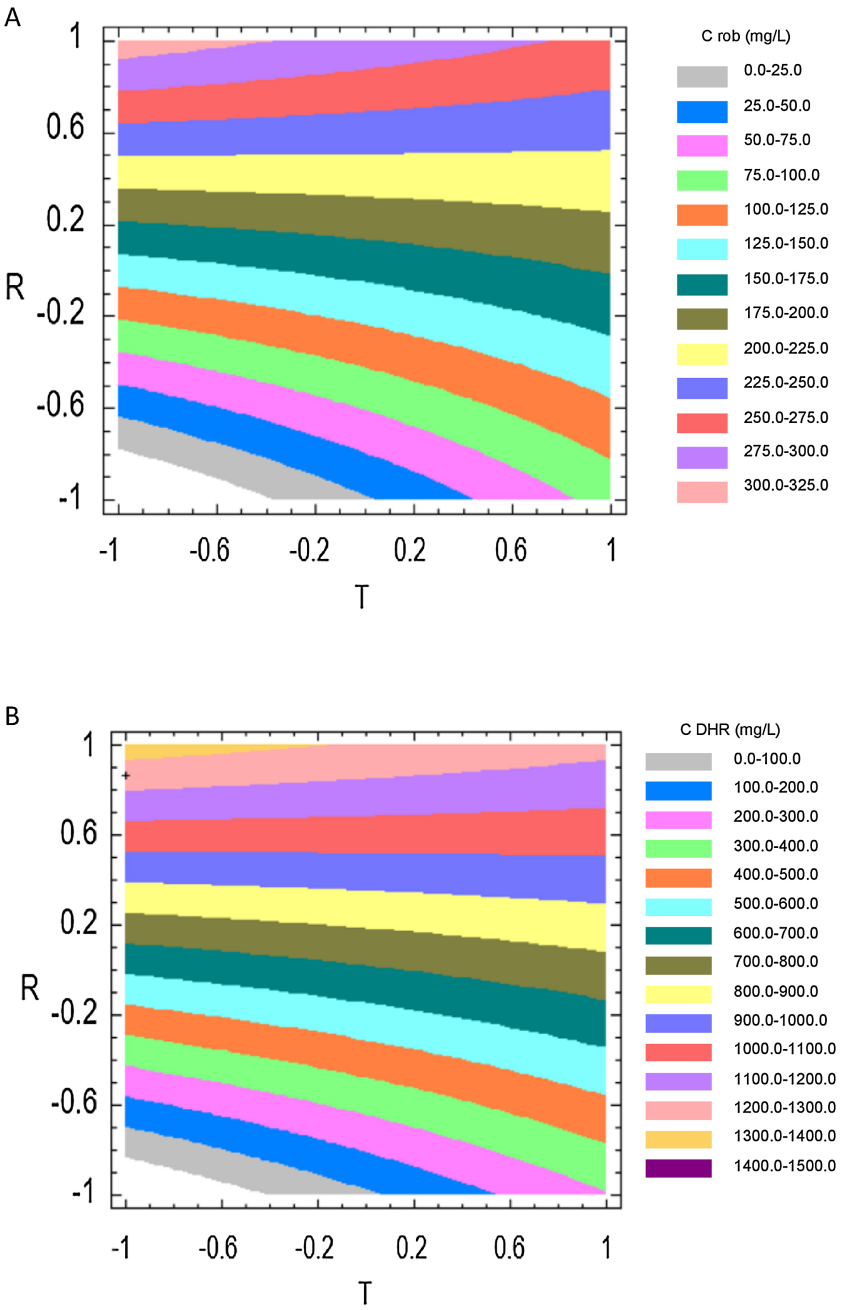

Fig. 5. 2D contour plot of temperature (*T*) versus solid/solvent weight ratio (*R*) on the extraction of DHR (A) and Robinetin (Rob) (B).

Table 3
F-test results of the quadratic polynomial model variables influencing Robinetin (Rob) concentration in the extracts.

Source[a]	Sum of squares	Df	Mean square	*F*-ratio	*p*-Value
T	1156.4	1	1156.4	0.90	0.4135
R	54,522.2	1	54,522.2	42.29	0.0074
TT	553.84	1	553.84	0.43	0.5590
TR	1317.69	1	1317.69	1.02	0.3865
RR	484.008	1	484.008	0.38	0.5834
Total error	3867.69	3	1289.23		
Corrected total	61,729.4	8			

r^2 = 94.7%
r^2_{adj} = 83.3%
[a] Studied variables: temperature (*T*); solid/solvent weight ratio (*R*).

the lack of fit and pure error is 19.00. This value is inferior to 19.19 corresponding to the tabulated value ($p = 0.05$; *3*; *2*) meaning that variances are identical. Nevertheless, the predicted coefficient of determination (r^2_{pred}) is equal to 0.72. Hence, the use of the model in view to calculate predictive values is limited. The pareto diagrams (Fig. 4A) confirms that temperature does not influence DHR extraction. This result is particularly interesting as it allows to conclude that an extraction performed at room temperature is statistically equivalent to an extraction performed at 40 °C. Hence, DHR extractions performed at room temperature will lower energy consumption and costs at an industrial level. Fig. 5A represents the response surface of DHR extraction according to *T* and *R*. One can observe that the lines are almost horizontal in the *T* direction due to the weak influence of this parameter. In the end, an estimated maximum concentration of extracted DHR would be

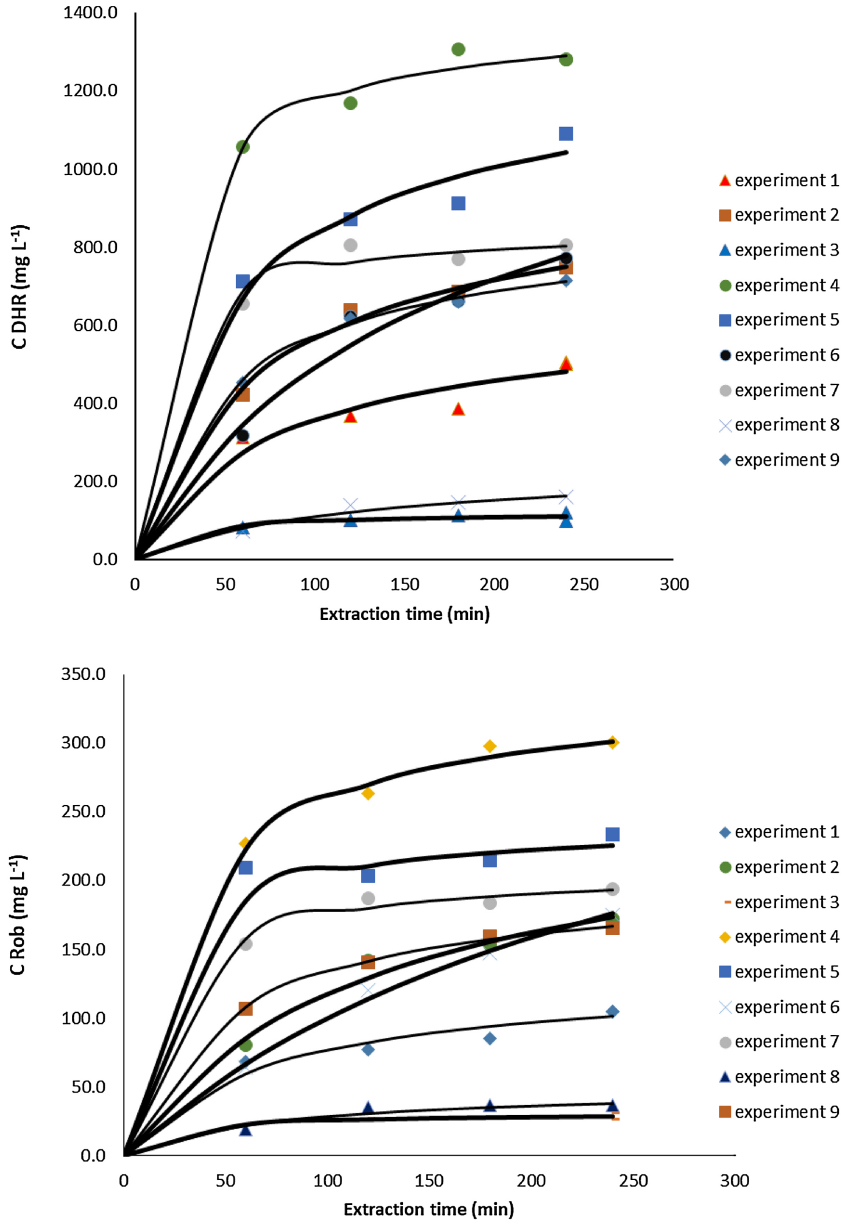

Fig. 6. Comparison of the experimental data obtained for solid–liquid extractions of dihydrorobinetin (DHR) and Robinetin (Rob) (plotted for each DoE experiment) with those calculated according to the kinetic model simulations (solid lines).

Table 4
Comparison between power law model and pseudo-second order rate model.

Experiment number	Pseudo-second order model				Power law model			
	r^2_{DHR}	$RMSD_{DHR}$	r^2_{Rob}	$RMSD_{Rob}$	r^2_{DHR}	$RMSD_{DHR}$	r^2_{Rob}	$RMSD_{Rob}$
1	0.913	38.0	0.947	6.9	0.847	29.3	0.890	4.6
2	0.992	18.2	0.964	7.0	0.944	31.5	0.931	10.3
3	0.940	7.9	0.966	1.4	0.601	7.6	0.716	1.2
4	0.997	29.5	0.998	5.3	0.919	30.7	0.972	5.7
5	0.970	48.0	0.990	13.6	0.944	35.1	0.474	8.1
6	0.912	40.6	0.966	3.4	0.922	54.2	0.982	6.0
7	0.995	29.0	0.997	4.8	0.717	34.1	0.847	6.3
8	0.925	9.7	0.937	2.7	0.889	13.3	0.823	3.6
9	0.998	10.3	0.999	1.5	0.960	20.6	0.973	4.2

Table 5
Kinetic modeling of dihydrorobinetin (DHR) and Robinetin (Rob) extraction: results of pseudo-second model application.

Experiment number	T (°C)	R (g g^{-1})	h_{DHR} (mg L^{-1} min^{-1})	Ce_{DHR} (mg L^{-1})	RD_{DHR} (2) (%)	h_{Rob} (mg L^{-1} min^{-1})	Ce_{Rob} (mg L^{-1})	RD_{Rob} (2) (%)
1	15.0	0.05	7.87	644.3	−21	1.79	134.0	−22
2	27.5	0.05	13.19	983.5	−24	2.10	265.0	−35
3	21.2	0.01	4.92	120.5	−1	1.37	31.2	−1
4	21.2	0.09	72.12	1394.2	−8	10.75	341.0	−12
5	33.8	0.09	23.22	1282.8	−15	13.05	242.6	−4
6	27.5	0.05	7.71	1345.4	−43	1.34	389.3	−55
7	40	0.05	59.31	850.2	−5	10.77	208.5	−7
8	33.8	0.01	1.95	251.3	−36	0.64	50.1	−28
9	27.5	0.05	16.21	870.2	−18	3.83	203.2	−19
Standard deviation (1)			4.68	265		1.25	102.7	

Data are calculated with experiments number: 2,6,9.
Relative deviation: $(C_{expi} - Ce_i)/Ce_i$ with i = Rob or DHR.

Table 6
Calculated extraction times to obtain 95% of the equilibrium concentration (Ce) for dihydrorobinetin (DHR) and Robinetin (Rob) for each experiment of the DoE.

Experiment number	$t_{(95,DHR)}$ (min)	$t_{(95,Rob)}$ (min)
1	1554	1398
2	1416	2395
3	476	434
4	367	603
5	1049	353
6	3314	5517
7	272	368
8	2437	1474
9	1020	1007

1400 mg L^{-1} within the studied domain for an optimized wood/solvent mass ration value of 0.9 (0.095 g g^{-1} or 74.9 g L^{-1}) and for reaction temperatures varying between −0.2 (25 °C) and −0.9 (16.5 °C), respectively.

3.1.2. Optimization of Rob extraction

The results of *F*-test concerning Rob extraction sources of variation are reported in Table 3 and also reveal that R is the only significant term. The same strategy as Section 3.1.1 was applied to determine the C_{Rob} extraction model and lead to the following relation: $C_{Rob} = 156.88 + 19.63T + 134.81R - 41RT$ with $r^2_{adj} = 0.877$ and $r^2 = 0.923$ (barely less descriptive than for DHR). In our hand however, the mean experimental errors are less important for C_{rob} than for C_{DHR} if we consider their respective coefficients of variation obtained for experiments 2, 6 and 9: 2.99% and 3.89%. C_{Rob} standard error of the model estimate is equal to 30.85 mg L^{-1} for a confidence interval of 12.75 mg L^{-1} with t ($p < 0.05$, 2). The *F*-ratio between the lack of fit and pure error is 59.53. This value is superior to 19.19 corresponding to tabulated value ($p = 0.05$; 3; 2) meaning in this case that lack of fit is more important that pure error. This is observed by value of standard error of the model higher than the confidence interval. Its predicted coefficient of determination (r^2_{pred}) is equal to 0.44. Hence, the use of model to calculate predictive values of C_{rob}, is rejected. As for DHR, the Pareto diagram shows that R is the most influent parameter for Rob extraction (Fig. 5B). However in this case, the second most important influencing parameter appears to be the interaction term (RT). Interestingly, the response surface of Rob extraction shows similitude with the DHR one (Fig. 6). Indeed, maximum Rob concentration (325 mg L^{-1}) is obtained in the same area for R values (R over 0.9 and T values between −0.2 and −1).

3.2. Kinetic modeling of Rob and DHR extraction

In the literature, several kinetic models are available to describe the release of target molecules from solid matters in solvents during solid–liquid extractions (for review: Sant'Anna et al., 2012). These models are: the power-law model, the Weibull type model, the two rates model, the swelling/diffusion model, the sorption/desorption model (also called pseudo-second order rate model), the pseudo-first model, and the Minchev and Minkov model. Finally, the general mass transfer model can also be applied (Wongkittipong et al., 2004). In order to apply the swelling/diffusion and pseudo-first order models, the equilibrium concentration needs to be known. In our study, a 4 h limit was applied. At the end of this time, the equilibrium concentration was not necessarily obtained (Fig. 6) discarding the use of this model. The Weibull type of model was also rejected due to the fact that the initial concentration at $t = 0$ min is supposed to be different from zero. Dutta et al. (2016) limited their studies to the pseudo first and second order models applied to batch extraction of seed oils from the fiber crop *Crotalaria juncea* (Sunn hemp). They showed that the pseudo-second order model lead to the highest r^2 value (0.97). Jurinjak Tušek et al. (2016) also showed that this model was the most representative compared to the two other tested (Weibull and logarithmic models). In the end, the pseudo-second order model was also used as a single modeling solution in other kinetic studies (Ho et al., 2005; Rakotondramasy-Rabesiaka et al., 2007; Su et al., 2014). In fact, solid–liquid extractions can be considered as the reverse operation of adsorption (Ho, 1995; Ho and McKay, 2000; Ho et al., 2005).

In the end, both power law and pseudo-second order models were tested to establish a kinetic description of C_{DHR} and C_{Rob} in the different experiments of the Doelhert design (Table 4). The r^2 estimations show that the pseudo-second order model is more descriptive for both molecules and every Doehlert experiments except for Exp. 6. The values of initial extraction rates and equilibrium concentration obtained according to this model are reported in Table 5. The curves corresponding to each model from Table 5 are confronted with our experimental data in Fig. 6. With r^2 higher than 0.9, they show that the pseudo-second model is indeed well descriptive of the extraction process for both molecules and for every experimental conditions tested. As one can notice, the initial extraction rate values (h) estimated are quite variable between experiments and range between 1.95 (Exp. 8) to 72.12 mg L^{-1}.min^{-1} (Exp. 4) and between 0.64 (Exp. 8) to 13.05 mg L^{-1} min^{-1} (Exp. 5) for DHR and Rob, respectively. In the case of equilibrium concentrations (C_e), the range is between 251.3 (Exp. 8) to 1392.2 mg L^{-1} (Exp. 4) and between 31.2 (Exp. 3) to 389.3 (Exp. 6) for DHR and Rob, respectively.

In Table 5, we were able to estimate for each experiment the relative deviation (RD) comparing the experimental concentrations measured after 4 h of extraction with the theoretical equilibrium concentrations calculated (C_e). Our results show that these RD are systematically negative suggesting that 4 h of extraction are globally insufficient to reach the equilibrium. In Table 6, the time to reach 95% of C_e is calculated by using Eq. (6). It allows us to appreciate the balance between reaching maximal concentrations of DHR and Rob and the time required to do it.

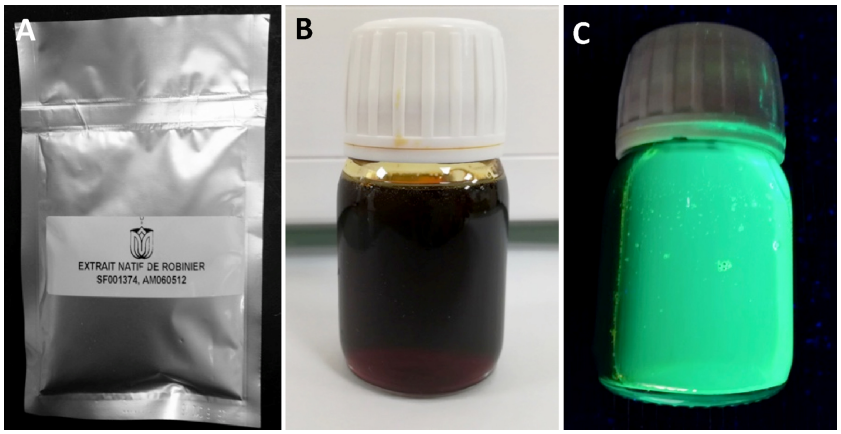

Fig. 7. Different types of *Robinia pseudoacacia* wood extracts were produced industrially. (A) Typical native extract batch containing dihydrorobinetin (DHR) (42%) and Rob (1.7% DW); (B and C) Robinia wood extract enriched in Robinetin (Rob) (9.2% DW) solubilized in 80% ethanol, observed under daylight and under U.V. light exposure (360 nm) equivalent to a standard "black light", respectively.

3.3. Evolution of the experimental design – simplex method

As visualized in Fig. 5, the highest concentrations of Rob and DHR are obtained for $R > 0.9$ at the limit of the studied domain suggesting that higher concentrations of both molecules could be obtained with conditions located outside of this domain. According to the Doehlert design properties and the previously described results, we applied the simplex method to complement this experimental plan in order to find optimal conditions (Fig. 1). Due to the fact that the best design border was for $R = 1$, we defined the initial simplex by associating the experimental points: 5, 4 and the central point corresponding to the experiments 2, 6 and 9. In this initial simplex, the central point corresponds to the less effective extraction conditions for R. According to Eq. (2) and for $\alpha = 1$, we determined the new experimental conditions (Exp. 10) to be tested (Fig. 1). For convenience, the results of the simplex complementary approach were added to those obtained through the Doelhert plan (Table 1 and Fig. 1). Exp. 10 allowed to increase the extraction efficiency of Rob and DHR from wood leading to C_{DHR} and C_{Rob} of 1782.1 mg L^{-1} and 398.4 mg L^{-1} in the extracts, respectively. In view of the results, an expansion of simplex 5, 4 and 10 was undertaken leading to experimental conditions 11. Upon completion of this experiment, C_{DHR} and C_{Rob} increased approximately by 1.7 fold in comparison with Exp. 10 confirming again a similar behavior for both molecules. Unfortunately, any further attempts to expand the simplex by increasing the value of R were not possible due to too high viscosities of the corresponding wood/solvent mixtures.

In the end, our results show that both molecules of interest characterizing *R. pseudoacacia* wood present similar responses toward the different extraction conditions that we have tested. In our hand, and considering the size of the wood particles used (0.4–1 mm), the optimal conditions determined for an efficient and simultaneous extraction of DHR and Rob correspond to those of Exp. 11 of the extended Doehlert plan ($T = 27.5$ °C; $R = 0.21$ g g^{-1} or 177 g L^{-1}). These conditions allowed us to obtain concentrated extracts of DHR and Rob of 2997.3 mg L^{-1} and 671.2 mg L^{-1}, respectively. Based on the volume of extract recovered at the end of the experimentation 11, the quantity of DHR and Rob extracted per gram of wood were estimated: 16 and 3.8, respectively. Sanz et al. (2011) reported higher yields of 32.3 mg g^{-1} and 7.8 mg g^{-1} for DHR and Rob, respectively. However, only heartwood presenting normally higher contents of extractives was used in this study. In addition, the wood particles used were of smaller sizes (0.28–0.80 mm) and also extracted for much longer time (24 h) with much more solvent ($R = 0.01$). Adapted to the limited timespan of 4 h corresponding to industrial requirements, our conditions were chosen as reference for scaling-up.

3.4. Industrial transfer

The DHR and Rob extraction conditions optimized in the laboratory were used to initiate an industrial production of *Robinia* wood extracts. Four pre-industrial pilot extractions were realized with about 50 kg of black locust wood each. The highest DHR and Rob contents within the different extracts obtained the different processes tested ranged between 35–42% and 9–11% (dry weight), respectively (Fig. 7). Initially, native industrial extracts (Fig. 7A) contained relatively lower amounts of Rob (1.5–2.5% dry weight) than those produced in the laboratory. Hence, the process was also adapted to produce extracts particularly enriched in Rob (Fig. 7B). These highly fluorescent extracts shows very promising perspectives for innovative applications in cosmetics (Fig. 7C). The biological properties of both types of extracts are currently being studied.

4. Conclusion

This study examined the effect of temperature and wood/solvent weight ratio on the extraction process of the two main extractives of *R. pseudoacacia* wood: robinetin and dihydrorobinetin. Our results show that wood/solvent mass (or volume) ratio was the most influent parameter and that the effect of temperature applied during the extraction process was negligible. The possibility to perform extractions at room temperature will insure minimal energy consumption during the foreseen industrial developments. Parallel evolutions of DHR and Rob concentrations during the extraction process also revealed that both molecules presented similar behaviours. The maximum concentrations obtained in the laboratory were about 3000 mg L^{-1} and 670 mg L^{-1} for dihydrorobinetin and robinetin, respectively. With r^2 superior to 0.91, kinetic results also showed that Rob and DHR extraction process are well described by pseudo-second order models. Modelling the extraction process showed that even though 4 h extractions did not allow us to reach DHR and Rob concentration equilibrium corresponding to maximum yields, this timespan represented a good compromise for an industrial production. In the end, we show that *R. pseudoacacia* wood represents a promising source of both of these flavonoids.

Acknowledgments

The authors thank the Région Centre-Val de Loire for financial support (ValRob project, APR 2012, grant number 00073766) and Eric De La Rochère (Arbocentre association, Orléans France) for supplying the wood used for the industrial pilots.

References

Barbier, C., Merzeau, D., Pastuszka, P., Charpentier, J.-P., 2016. Une première collection nationale de robiniers. Forêt-Entreprise 226, 10–19.

Benesperi, R., Giuliani, C., Zanetti, S., Gennai, M., Mariotti Lippi, M., Guidi, T., Nascimbene, J., Foggi, B., 2012. Forest plant diversity is threatened by *Robinia pseudoacacia* (black-locust) invasion. Biodivers. Conserv. 21, 3555–3568. https://doi.org/10.1007/s10531-012-0380-5.

Bezerra, M.A., Santelli, R.E., Oliveira, E.P., Villar, L.S., Escaleira, L.A., 2008. Response surface methodology (RSM) as a tool for optimization in analytical chemistry. Talanta 76, 965–977. https://doi.org/10.1016/j.talanta.2008.05.019.

Bostyn, S., Cagnon, B., Fauduet, H., 2009. Optimization by the simplex method of the separation of phenolic acids by high-performance liquid chromatography in wastewater olive and sugar beet vinasse. Talanta 80, 1–7. https://doi.org/10.1016/j.talanta.2009.06.040.

Chartier, A., Beaumesnil, M., de Oliveira, A.L., Elfakir, C., Bostyn, S., 2013. Optimization of the isolation and quantitation of kahweol and cafestol in green coffee oil. Talanta 117, 102–111. https://doi.org/10.1016/j.talanta.2013.07.053.

D'Attoma, J., Camara, T., Brun, P.L., Robin, Y., Bostyn, S., Buron, F., Routier, S., 2017. Efficient transposition of the sandmeyer reaction from batch to continuous process. Org. Process Res. Dev. 21, 44–51. https://doi.org/10.1021/acs.oprd.6b00318.

Destandau, E., Charpentier, J.-P., Bostyn, S., Zubrzycki, S., Serrano, V., Seigneuret, J.-M., Breton, C., 2016. Gram-scale purification of dihydrorobinetin from *Robinia pseudoacacia* L. wood by centrifugal partition chromatography. Separations 3, 23. https://doi.org/10.3390/separations3030023.

Dutta, R., Sarkar, U., Mukherjee, A., 2016. Pseudo-kinetics of batch extraction of *Crotalaria juncea* (Sunn hemp) seed oil using 2-propanol. Ind. Crop Prod. 87, 9–13. https://doi.org/10.1016/j.indcrop.2016.04.006.

George, V.C., Dellaire, G., Rupasinghe, H.P.V., 2017. Plant flavonoids in cancer chemoprevention: role in genome stability. J. Nutr. Biochem. 45, 1–14. https://doi.org/10.1016/j.jnutbio.2016.11.007.

Guharay, J., Sengupta, P.K., 1997. Excited-state proton-transfer and dual fluorescence of robinetin in different environments. Spectrochim. Acta A: Mol. Biomol. Spectrosc. 53, 905–912. https://doi.org/10.1016/S1386-1425(97)89475-9.

Hillis, W.E., 1987. Heartwood and Tree Exudates. Springer-Verlag, Berlin, Germany, pp. 268.

Ho, Y.S., 1995. Adsorption of heavy metals from waste streams by peat (Ph.D. Thesis). University of Birmingham, UK.

Ho, Y.S., McKay, G., 2000. The kinetics of sorption of divalent metal ions onto sphagnum moss peat. Water Res. 34 (3), 735–742. https://doi.org/10.1016/S0043-1354(99)00232-8.

Ho, Y.S., Adamou, H.O.H., Fauduet, H., Porte, C., 2005. Kinetics and model building of leaching of water-soluble compounds of *Tilia* sapwood. Sep. Purif. Technol. 45, 169–173. https://doi.org/10.1016/j.seppur.2005.03.007.

Jurinjak Tušek, A., Benković, M., Belščak Cvitanović, A., Valinger, D., Jurina, T., Gajdoš Kljusurić, J., 2016. Kinetics and thermodynamics of the solid–liquid extraction process of total polyphenols, antioxidants and extraction yield from *Asteraceae* plants. Ind. Crop Prod. 91, 205–214. https://doi.org/10.1016/j.indcrop.2016.07.015.

Katsampa, P., Valsamedou, E., Grigorakis, S., Makris, D.P., 2015. A green ultrasound-assisted extraction process for the recovery of antioxidant polyphenols and pigments from onion solid wastes using Box–Behnken experimental design and kinetics. Ind. Crop Prod. 77, 535–543. https://doi.org/10.1016/j.indcrop.2015.09.039.

Magel, E., Jay-Allemand, C., Ziegler, H., 1994. Formation of heartwood substances in the stemwood of *Robinia pseudoacacia* L. II. Distribution of nonstructural carbohydrates and wood extractives across the trunk. Trees 8, 165–171. https://doi.org/10.1007/BF00196843.

Magel, E., 2000. Biochemistry and physiology of heartwood formation. In: Savidge, R., Barnett, J., Napier, R. (Eds.), Molecular and Cell Biology of Wood Formation. BIOS Scientific Publishers Ltd., Oxford, pp. 363–376.

Mkaouar, S., Gelicus, A., Bahloul, N., Allaf, K., Kechaou, N., 2016. Kinetic study of polyphenols extraction from olive (*Olea europaea* L.) leaves using instant controlled pressure drop texturing. Sep. Purif. Technol. 161, 165–171. https://doi.org/10.1016/j.seppur.2016.02.002.

Moreno-Vilet, L., Bonnin-Paris, J., Bostyn, S., Ruiz-Cabrera, M.A., Moscosa-Santillán, M., 2014. Assessment of sugars separation from a model carbohydrates solution by nanofiltration using a design of experiments (DoE) methodology. Sep. Purif. Technol. 131, 84–93. https://doi.org/10.1016/j.seppur.2014.04.040.

Odabaş, H.İ., Koca, I., 2016. Application of response surface methodology for optimizing the recovery of phenolic compounds from hazelnut skin using different extraction methods. Ind. Crop Prod. 91, 114–124. https://doi.org/10.1016/j.indcrop.2016.05.033.

Patil, D.M., Akamanchi, K.G., 2017. Ultrasound-assisted rapid extraction and kinetic modelling of influential factors: extraction of camptothecin from Nothapodytes nimmoniana plant. Ultrason. Sonochem. 37, 582–591. https://doi.org/10.1016/j.ultsonch.2017.02.015.

Peleg, M., 1988. An empirical model for the description of moisture sorption curves. J. Food Sci. 53, 1216–1219. https://doi.org/10.1111/j.1365-2621.1988.tb13565.x.

Rakotondramasy-Rabesiaka, L., Havet, J.-L., Porte, C., Fauduet, H., 2007. Solid–liquid extraction of protopine from *Fumaria officinalis* L.—analysis determination, kinetic reaction and model building. Sep. Purif. Technol. 54, 253–261.

Sant'Anna, V., Brandelli, A., Marczak, L.D.F., Tessaro, I.C., 2012. Kinetic modeling of total polyphenol extraction from grape marc and characterization of the extracts. Sep. Purif. Technol. 100, 82–87. https://doi.org/10.1016/j.seppur.2012.09.004.

Sanz, M., Fernández de Simón, B., Esteruelas, E., Muñoz, Á.M., Cadahía, E., Hernández, T., Estrella, I., Pinto, E., 2011. Effect of toasting intensity at cooperage on phenolic compounds in acacia (*Robinia pseudoacacia*) heartwood. J. Agric. Food Chem. 59, 3135–3145. https://doi.org/10.1021/jf1042932.

Scheffer, T.C., Cowling, E.B., 1966. Natural resistance of wood to microbial deterioration. Annu. Rev. Phytopathol. 4, 147–168. https://doi.org/10.1146/annurev.py.04.090166.001051.

Sergent, T., Kohnen, S., Jourez, B., Beauve, C., Schneider, Y.-J., Vincke, C., 2014. Characterization of black locust (*Robinia pseudoacacia* L.) heartwood extractives: identification of resveratrol and piceatannol. Wood Sci. Technol. 48, 1005–1017. https://doi.org/10.1007/s00226-014-0656-x.

Shain, L., 1977. The effects of extractives from black locust heartwood on *Fomes rimosus* and other decay fungi. Proc. Am. Phytopath. Soc. 3, 216.

Spendley, W., Hext, G.R., Himsworth, F.R., 2012. Sequential application of simplex designs in optimisation and evolutionary operation. Technometrics 4, 441–461. https://doi.org/10.1080/00401706.1962.10490033.

Su, C.-H., Liu, C.-S., Yang, P.-C., Syu, K.-S., Chiuh, C.-C., 2014. Solid–liquid extraction of phycocyanin from *Spirulina platensis*: Kinetic modeling of influential factors. Sep. Purif. Technol. 123, 64–68. https://doi.org/10.1016/j.seppur.2013.12.026.

Weber, E., Gut, D., 2004. Assessing the risk of potentially invasive plant species in central Europe. J. Nat Conserv. 12, 171–179. https://doi.org/10.1016/j.jnc.2004.04.002.

Wongkittipong, R., Prat, L., Damronglerd, S., Gourdon, C., 2004. Solid–liquid extraction of andrographolide from plants—experimental study, kinetic reaction and model. Sep. Purif. Technol. 4, 147–154. https://doi.org/10.1016/j.seppur.2004.02.002.